

# BiFeO<sub>3</sub> Crystal Structure at Low Temperatures

A. PALEWICZ<sup>a</sup>, I. SOSNOWSKA<sup>a</sup>, R. PRZENIOSŁO<sup>a</sup> AND A.W. HEWAT<sup>b</sup>

<sup>a</sup>Institute of Experimental Physics, Faculty of Physics, University of Warsaw  
Hoża 69, 00-681 Warsaw, Poland

<sup>b</sup>Institut Laue Langevin, 6 rue J. Horowitz, 38042 Grenoble, France

The crystal and magnetic structure of BiFeO<sub>3</sub> have been studied with the use of high resolution neutron diffraction between 5 K and 300 K. The atomic coordinates in BiFeO<sub>3</sub> are almost unchanged between 5 K and 300 K.

PACS numbers: 61.05.fm, 61.66.Fn, 75.50.Ee, 77.84.Bw

## 1. Introduction

BiFeO<sub>3</sub> is an important material because of its multiferroic properties: a simultaneous electric polarization below 1100 K [1] and a long range magnetic order below 640 K [2–5]. The main motivation of the studies of the electronic and magnetic properties of BiFeO<sub>3</sub> is due to potential applications of the magnetoelectric coupling at temperatures around room temperature (RT) [6–9].

Early studies of BiFeO<sub>3</sub> single crystals reported a relatively weak polarization values around 6.1  $\mu\text{C}/\text{cm}^2$  [1]. A significant increase of the polarization up to 60  $\mu\text{C}/\text{cm}^2$  was reported in BiFeO<sub>3</sub> strained thin films [10]. It has been shown recently that high values of the electric polarization around 70  $\mu\text{C}/\text{cm}^2$  can be also observed in thin films without large strains [11]. Similar polarization values were also observed recently in high quality BiFeO<sub>3</sub> single crystals [12] and in ceramic samples [13]. It is therefore important to distinguish the effects due to changes of the crystal structure of bulk BiFeO<sub>3</sub> from effects due to sample morphologies, like strains, impurities, grain boundaries, etc. . . These recent results underline the importance of a precise knowledge of the bulk BiFeO<sub>3</sub> crystal structure in a wide temperature range. A schematic presentation of the BiFeO<sub>3</sub> unit cell and the ordering of the Fe<sup>3+</sup> magnetic moments is shown in Fig. 1.

Important changes of the Raman spectra observed in BiFeO<sub>3</sub> single crystals at  $T^* = 550$  K [14] and a maximum of the thermal expansion coefficient near 640 K [15, 16] suggest a strong spin-lattice coupling.

Recently, a number of BiFeO<sub>3</sub> studies have shown important phenomena also at temperatures below RT. The spontaneous polarization of a single crystal BiFeO<sub>3</sub> shows quite unusual temperature behaviour with two local maxima (with opposite signs) near 100 K and 200 K, as shown in Refs. [18, 19]. Another study has shown a considerable increase of the low frequency permittivity and dielectric loss in BiFeO<sub>3</sub> between 150 K and 200 K [20]. There are also changes of the Fe nuclear magnetic resonance (NMR) signal reported at RT and at 100 K [21], and anomalies of the Raman spectra near 140 K and 200 K

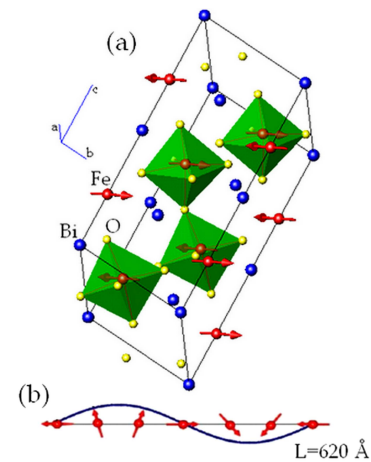


Fig. 1. (a) Schematic presentation of the BiFeO<sub>3</sub> unit cell in the hexagonal setting of space group  $R3c$ . The Bi, Fe and O ions are shown with blue, red and yellow symbols, respectively. The distorted FeO<sub>6</sub> octahedra are shown in green. The (almost) antiparallel Fe<sup>3+</sup> magnetic moments are shown with red arrows. The lower part of the figure (b) shows that the magnetic moments' direction changes in a periodic way [3].

[22–24], as well as, elastic and electrical anomalies [25]. On the other hand, recent BiFeO<sub>3</sub> magnetic [26, 27], dielectric and heat capacity [27] studies do not show any anomalies below RT. All these important phenomena motivated us to study the changes of structural parameters of BiFeO<sub>3</sub> at temperatures below RT by using high resolution neutron diffraction.

## 2. Experimental

The ceramic BiFeO<sub>3</sub> sample was prepared using a procedure described by Achenbach et al. [28]. Neutron powder diffraction measurements of BiFeO<sub>3</sub> were performed by using the diffractometer D2B at the Institut Laue Langevin (ILL) Grenoble, operating at the neutron wavelength of 1.5944(1) Å in a similar setup as described in our previous paper [17]. The powder BiFeO<sub>3</sub> sam-

ple was placed in vanadium container 8 mm in diameter and mounted in a closed cycle refrigerator. The measurements were performed at several temperatures between 5 K and RT, with 25 K intervals. Neutron powder diffraction patterns for BiFeO<sub>3</sub> were analyzed by the Rietveld method [29] using the refinement program FullProf [30]. The wavelength calibration and instrumental resolution were determined by using the diffraction pattern of a reference CeO<sub>2</sub> sample measured in the same experimental setup. We used the pseudo-Voigt peakshape and the background was interpolated between 14 points. The agreement factors and  $2\theta$  zero shifts are summarized in Table I.

TABLE I  
Summary of the Rietveld refinement agreement factors and  $2\theta$  zero shifts.

Temperature range	5–298 K
$R_p$ [%]	4.24–4.94
$R_{wp}$ [%]	5.98–6.79
$R_{exp}$ [%]	4.72–4.81
$R_{mag}$ [%]	2.08–2.69
$R_{Bragg}$ [%]	4.56–5.16
$\chi^2$	1.55–2.07
$2\theta$ zero shift	0.1418(14)–0.1439(14)

### 3. Results

The neutron powder diffraction pattern collected between 5 K and RT shows Bragg peaks, which agree with the BiFeO<sub>3</sub> crystal structure described by the space

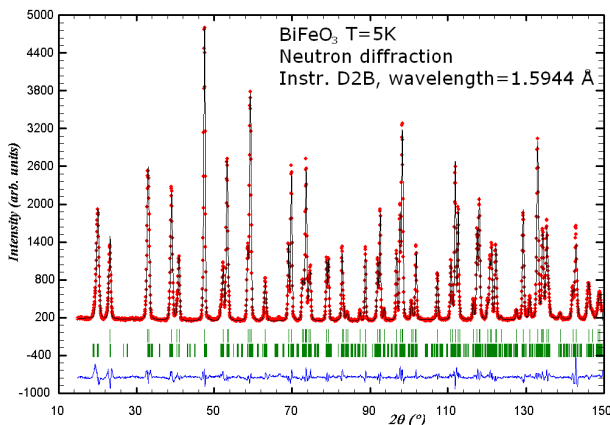


Fig. 2. Results of the Rietveld refinement of the neutron powder diffraction pattern of BiFeO<sub>3</sub> measured at 5 K. The measured data and the calculated diffraction pattern are represented by solid circles and solid line, respectively. Below the graph there is shown a difference curve. The ticks indicate positions of the Bragg peaks owing to crystal (upper ticks) and magnetic (lower ticks) structures of BiFeO<sub>3</sub>.

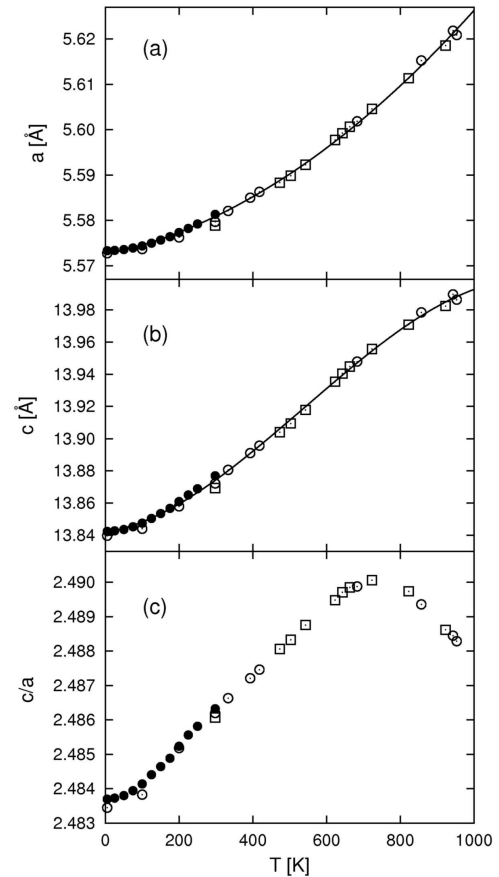


Fig. 3. Temperature dependences of the BiFeO<sub>3</sub> lattice constants  $a$  and  $c$ , and their ratio — determined from the present neutron diffraction data (solid circles), previous neutron diffraction data [17] (empty squares) and previous SR studies (empty circles) [34]. The fitted polynomials are shown as solid lines in (a) and (b).

group  $R3c$  [2, 17, 31–33]. There are four positional parameters to be determined:  $z_{Fe}$ ,  $x_O$ ,  $y_O$  and  $z_O$  [2]. Anisotropic displacement factors were refined for all the ions in BiFeO<sub>3</sub> structure as it has been already done in Refs. [17, 31]. The results of the Rietveld refinement of the BiFeO<sub>3</sub> neutron powder diffraction pattern at  $T = 5$  K are shown in Fig. 2.

The lattice parameters of BiFeO<sub>3</sub> determined from our measurements, shown in Fig. 3, agree with the values determined recently from a high resolution synchrotron radiation (SR) diffraction [34]. Present studies were performed at more temperatures as compared with earlier ones [34]. The observed temperature dependence can be described with polynomials:

$$a(T) = 5.57249 + 1.70872 \times 10^{-5}T + 3.67303 \times 10^{-8}T^2 \quad (1)$$

$$c(T) = 13.84189 + 3.53563 \times 10^{-5}T + 2.99348 \times 10^{-7}T^2 - 1.839294 \times 10^{-10}T^3. \quad (2)$$

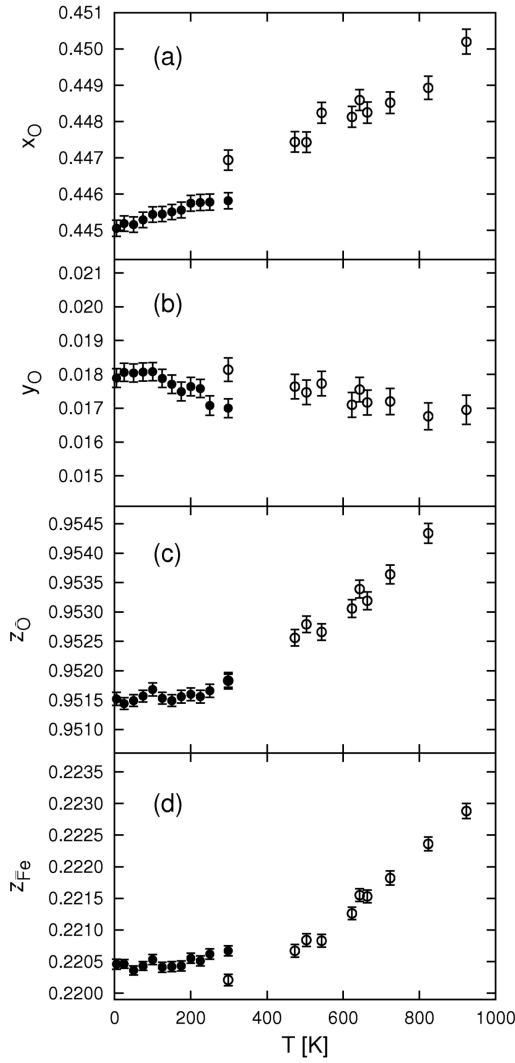


Fig. 4. Temperature dependence of the fractional atomic coordinates for  $\text{BiFeO}_3$  obtained from a high resolution neutron diffraction data. The values of  $x_{\text{O}}$ ,  $y_{\text{O}}$ ,  $z_{\text{O}}$  and  $z_{\text{Fe}}$  are shown in panels (a), (b), (c) and (d), respectively. Present data (full symbols) are shown with data from Ref. [17] (empty symbols).

The low-temperature dependence of positional parameters  $x_{\text{O}}$ ,  $y_{\text{O}}$ ,  $z_{\text{O}}$  and  $z_{\text{Fe}}$ , obtained from the present data, are shown together with results from the high-temperature studies [17] in Fig. 4. The  $x_{\text{O}}$  position slightly increases with temperature, while  $y_{\text{O}}$  remains almost constant. The most interesting is the behaviour of  $z_{\text{O}}$  and  $z_{\text{Fe}}$  positions, which are both almost constant below RT and they both increase considerably above RT. The results at RT do not coincide exactly but they show similar values and they are close to the results from Refs. [2, 31]. It is important to note that the  $\text{BiFeO}_3$  unit cell polarization depends on the  $z$  atomic coordinates. There are two Bi–Fe distances along the hexagonal  $c$ -axis, one is shorter ( $l_1 = z_{\text{Fe}} \times c$ ) and the other is longer ( $l_2 = (1/2 - z_{\text{Fe}}) \times c$ ). Temperature dependences of both

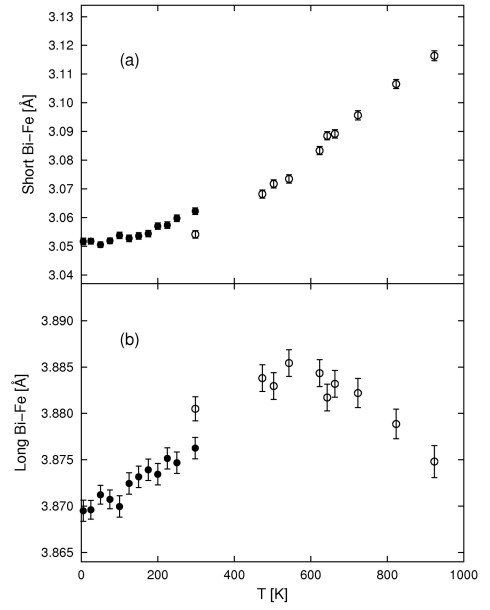


Fig. 5. Temperature dependences of the short ( $l_1$ ) and long ( $l_2$ ) Bi–Fe distances along the  $c$ -axis, determined from high resolution neutron diffraction data. Present data (full symbols) are shown with data from Ref. [17] (empty symbols).

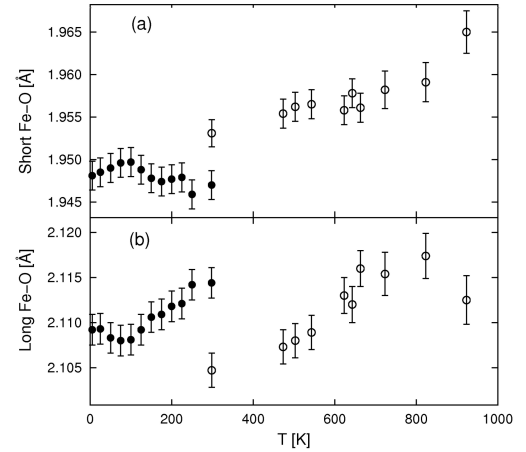


Fig. 6. Temperature dependence of the short and long Fe–O bond lengths determined from a high resolution neutron diffraction data. Present data (full symbols) are shown with data from Ref. [17] (empty symbols).

$l_1$  and  $l_2$  are shown in Fig. 5. The long Bi–Fe distance shows a clear maximum near  $T^* \approx 550$  K where Raman spectra anomalies were reported [14]. The temperature dependence of Fe–O bond lengths and of O–Fe–O, Fe–O–Fe bond angles are shown in Figs. 6 and 7, respectively. The O–Fe–O is an angle inside the  $\text{FeO}_6$  octahedron.

The magnetic ordering of  $\text{Fe}^{3+}$  magnetic moments in  $\text{BiFeO}_3$  is modulated with a long period of  $620 \text{ \AA}$  [3–5], but the splitting of magnetic satellite peaks was not ob-

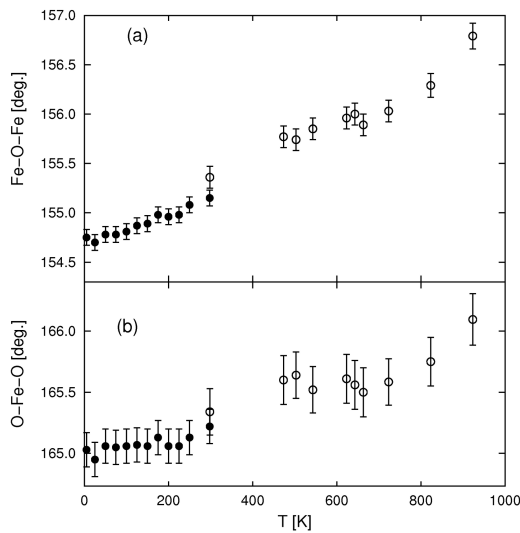


Fig. 7. Temperature dependence of the Fe–O–Fe and O–Fe–O bond angles determined from a high resolution neutron diffraction data. Present data (full symbols) are shown with data from Ref. [17] (empty symbols).

served in the present measurements. The data was refined by assuming an antiferromagnetic *G*-type ordering of Fe<sup>3+</sup> magnetic moments with an arbitrary direction taken along the hexagonal *a* axis. This model gives the same reliability factors as compared with the modulated magnetic ordering [3]. The temperature dependence of the magnetic (101) + (003) to nuclear (024) Bragg peaks intensity ratio (Fig. 8) shows weak changes below RT, in agreement with Ref. [2].

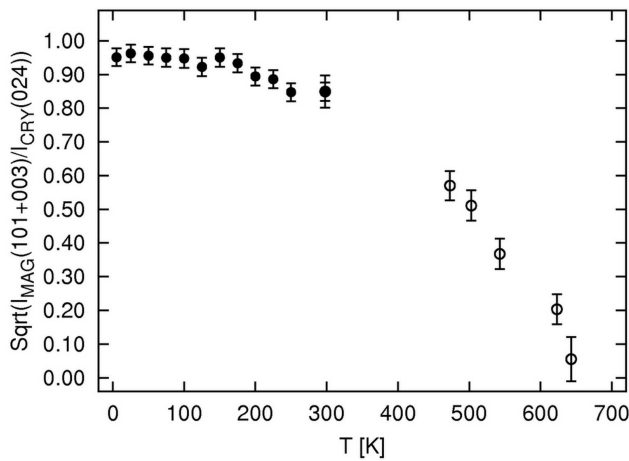


Fig. 8. Temperature dependence of the square root of the intensity ratio between merged magnetic Bragg peaks (101) + (003) and nuclear (024) Bragg peak. Present data (full symbols) are shown with data from Ref. [17] (empty symbols).

The anisotropy of the atomic displacement factors, observed already in BiFeO<sub>3</sub> studies above RT [17], are also significant at low temperatures down to 5 K. A fit with the *T* = 5 K data, assuming different isotropic displacement factors for Bi, Fe and O ions, gives the Bragg factor:  $R_B = 3.91\%$ . A fit to the same data, assuming anisotropic displacement factors for Bi, Fe and O ions, gives a smaller Bragg factor:  $R_B = 3.52\%$ . The anisotropy of the atomic displacement factors is most pronounced for O ions.

At temperatures below 150 K we obtained negative values of atomic displacements *B* for Bi and Fe indicating a systematic error in intensity vs. scattering angle, that could be produced by neutron absorption. However, the neutron absorption of the polycrystalline BiFeO<sub>3</sub> sample and of the vanadium container was estimated to be only  $\mu R = 0.017$ , which is insufficient to explain the negative atomic displacement factors for Bi and Fe ions at temperatures below 150 K. For comparison, a calibration data with a reference CeO<sub>2</sub> sample was obtained in the same experimental setup and refined assuming the crystal structure given in Ref. [35]. The refined atomic displacement parameters (ADPs) for CeO<sub>2</sub>:  $B_{Ce} = 0.27(5) \text{ \AA}^2$  and  $B_O = 0.36(4) \text{ \AA}^2$  are considerably smaller than the values from Ref. [35]:  $B_{Ce} = 0.46(5) \text{ \AA}^2$  and  $B_O = 0.76(4) \text{ \AA}^2$ . These results suggest that there is a similar systematic error in intensity vs. angle for BiFeO<sub>3</sub>, as well as, for the CeO<sub>2</sub> standard sample. By applying a systematic shift of  $0.2 \text{ \AA}^2$  to  $B_{equiv}$  upwards one gets an agreement with the results obtained earlier [2], i.e.,  $B = 0.07(9) \text{ \AA}^2$  at 4 K and  $B = 0.56(9) \text{ \AA}^2$  at 293 K. The temperature dependences of the atomic displacement factor  $B_{equiv}$  to the anisotropic ADPs for Bi, Fe and O ions are shown in Fig. 9.

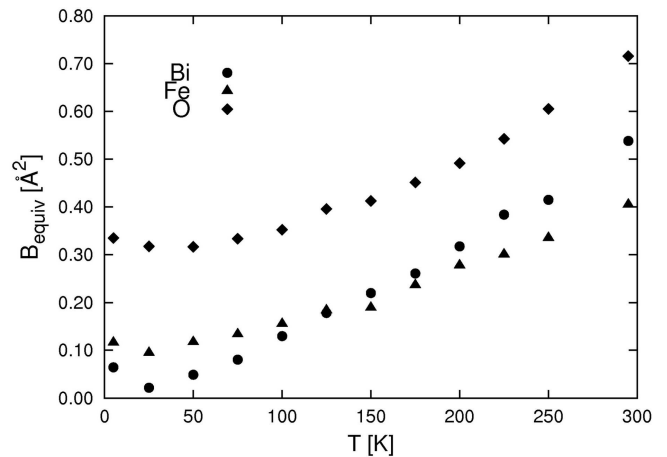


Fig. 9. Temperature dependence of the atomic displacement factor  $B_{equiv}$  for Bi, Fe, and O ions in BiFeO<sub>3</sub>, determined from a high resolution neutron diffraction data.

TABLE II

(Supporting Information) Values of the structural parameters of BiFeO<sub>3</sub>.  $T$  stands for temperature,  $a$  and  $c$  are the lattice constants (in the hexagonal setting of space group  $R3c$ );  $z_{\text{Fe}}$ ,  $x_{\text{O}}$ ,  $y_{\text{O}}$  and  $z_{\text{O}}$  are the fractional coordinates of the Fe<sup>3+</sup> and Bi<sup>3+</sup> ions, respectively. The Fe–Bi and Fe–O bond lengths, as well as O–Fe–O and Fe–O–Fe bond angles are presented.

T [K]	a [Å]	c [Å]	$z_{\text{Fe}}$	$x_{\text{O}}$	$y_{\text{O}}$	$z_{\text{O}}$
5	5.57330(5)	13.84238(16)	0.22046(8)	0.44506(22)	0.01789(28)	0.95152(11)
25	5.57338(5)	13.84277(15)	0.22046(7)	0.44519(21)	0.01806(27)	0.95144(10)
50	5.57355(5)	13.84359(15)	0.22036(7)	0.44516(21)	0.01804(27)	0.95149(10)
75	5.57391(5)	13.84528(15)	0.22043(7)	0.44529(21)	0.01807(27)	0.95157(10)
100	5.57436(5)	13.84749(15)	0.22053(8)	0.44544(21)	0.01808(27)	0.95168(11)
125	5.57495(5)	13.85044(15)	0.22041(8)	0.44545(21)	0.01788(27)	0.95153(10)
150	5.57564(5)	13.85348(15)	0.22042(8)	0.44551(21)	0.01771(27)	0.95149(10)
175	5.57639(5)	13.85669(15)	0.22043(8)	0.44556(22)	0.01749(28)	0.95156(11)
200	5.57731(5)	13.86092(15)	0.22055(8)	0.44575(22)	0.01764(27)	0.95160(11)
225	5.57823(5)	13.86504(15)	0.22051(8)	0.44577(22)	0.01758(27)	0.95156(11)
250	5.57920(5)	13.86886(15)	0.22062(8)	0.44578(22)	0.01708(29)	0.95166(11)
298	5.58132(5)	13.87698(15)	0.22067(8)	0.44582(22)	0.01700(28)	0.95183(11)
T [K]	Fe–Bi (1) [Å]	Fe–Bi (2) [Å]	Fe–O (1) [Å]	Fe–O (2) [Å]	O–Fe–O [deg]	Fe–O–Fe [deg]
5	3.0517(11)	3.8695(12)	1.9481(17)	2.1092(17)	165.03(14)	154.75(8)
25	3.0518(10)	3.8696(10)	1.9485(17)	2.1093(17)	164.95(14)	154.70(8)
50	3.0506(10)	3.8712(10)	1.9490(17)	2.1083(17)	165.06(14)	154.78(8)
75	3.0519(11)	3.8707(10)	1.9496(17)	2.1080(17)	165.05(14)	154.78(8)
100	3.0538(11)	3.8700(12)	1.9497(17)	2.1081(17)	165.06(14)	154.81(8)
125	3.0528(11)	3.8724(11)	1.9488(17)	2.1092(17)	165.07(14)	154.87(8)
150	3.0536(11)	3.8732(12)	1.9478(17)	2.1106(17)	165.06(14)	154.89(8)
175	3.0544(11)	3.8739(12)	1.9474(17)	2.1109(17)	165.13(14)	154.98(8)
200	3.0570(11)	3.8734(12)	1.9477(17)	2.1118(17)	165.06(14)	154.96(8)
225	3.0574(11)	3.8751(12)	1.9479(17)	2.1121(17)	165.06(14)	154.98(8)
250	3.0597(11)	3.8747(12)	1.9459(17)	2.1142(17)	165.13(14)	155.08(8)
298	3.0622(11)	3.8763(11)	1.9470(17)	2.1144(17)	165.22(14)	155.15(8)

#### 4. Conclusions

Temperature dependence of the BiFeO<sub>3</sub> structural parameters was determined by neutron powder diffraction below RT. The present study shows that there is little change in the fractional atomic coordinates in the unit cell of BiFeO<sub>3</sub> between 5 K and 300 K. The  $z$  atomic coordinates of Fe and O ions, which determine the BiFeO<sub>3</sub> unit cell polarization, increase considerably above 300 K. The various phenomena reported in the literature for this temperature regime can not then be connected with changes of the crystal structure of BiFeO<sub>3</sub>. Our present results are in agreement with recent BiFeO<sub>3</sub> studies, which also do not show any anomalies below RT.

#### Acknowledgments

This work was supported by the Ministry of Science and Higher Education (Poland). The ILL Grenoble is

acknowledged for giving access to neutron scattering facilities.

#### References

- [1] J.R. Teague, R. Gerson, W.J. James, *Solid State Comm.* **8**, 1073 (1970).
- [2] P. Fischer, M. Połomska, I. Sosnowska, M. Szymański, *J. Phys C* **13**, 1931 (1980).
- [3] I. Sosnowska, T. Peterlin-Neumaier, E. Steichele, *J. Phys C* **15**, 4835 (1982).
- [4] I. Sosnowska, M. Loewenhaupt, W.I.F. David, R.M. Ibberson, *Physica B* **180-181**, 117 (1992).
- [5] R. Przeniosło, A. Palewicz, M. Regulski, I. Sosnowska, R.M. Ibberson, K.S. Knight, *J. Phys., Condens. Matter* **18**, 2069 (2006).
- [6] M. Fiebig, *J. Phys. D, Appl. Phys.* **38**, R123 (2005).
- [7] N.A. Hill, *J. Phys. Chem. B* **104**, 6694 (2000).
- [8] G. Catalan, J.F. Scott, *Adv. Mater.* **21**, 2463 (2009).

- [9] J.F. Scott, *J. Magn. Magn. Mater.* **321**, 1689 (2009).
- [10] J. Wang, J.B. Neaton, H. Zheng, V. Nagarajan, S.B. Ogale, B. Liu, D. Viehland, V. Vaithyanathan, D.G. Schlom, U.V. Waghmare, N.A. Spaldin, K.M. Rabe, M. Wuttig, R. Ramesh, *Science* **299**, 1719 (2003).
- [11] K.Y. Yun, M. Noda, M. Okuyama, *Appl. Phys. Lett.* **83**, 3981 (2003).
- [12] D. Lebeugle, D. Colson, A. Forget, M. Viret, P. Bonville, J.F. Marucco, S. Fusil, *Phys. Rev. B* **76**, 024116 (2007).
- [13] V.V. Shvartsman, W. Kleemann, R. Haumont, J. Kreisel, *Appl. Phys. Lett.* **90**, 172115 (2007).
- [14] R. Haumont, J. Kreisel, P. Bouvier, F. Hippert, *Phys. Rev. B* **73**, 132101 (2006).
- [15] R. Mazumder, S. Ghosh, P. Mondal, D. Bhattacharya, S. Dasgupta, N. Das, A. Sen, A.K. Tyagi, M. Sivakumar, T. Takami, H. Ikuta, *J. Appl. Phys.* **100**, 033908 (2006).
- [16] A.A. Amirov, A.B. Batdalov, S.N. Kallaev, Z.M. Omarov, I.A. Verbenko, O.N. Razumovskaya, L.A. Reznichenko, L.A. Shilkina, *Phys. Sol. Stat.* **51**, 1189 (2009).
- [17] A. Palewicz, R. Przeniosło, I. Sosnowska, A.W. Hewat, *Acta Cryst. B* **63**, 537 (2007).
- [18] Yu.V. Shaldin, S. Matyjasik, *Doklady Physics* **51**, 397 (2006).
- [19] Yu.V. Shaldin, S. Matyjasik, A.A. Bush, *Crystallography Reports* **52**, 123 (2007).
- [20] S. Kamba, D. Nuzhnyy, M. Savinov, J. Šebek, J. Petzelt, J. Prokleška, R. Haumont, J. Kreisel, *Phys. Rev. B* **75**, 024403 (2007).
- [21] A.V. Zalessky, A.A. Frolov, T.A. Khimich, A.A. Bush, V.S. Pokatilov, A.K. Zvezdin, *Europhys. Lett.* **50**, 547 (2000).
- [22] M.K. Singh, R.S. Katiyar, J.F. Scott, *J. Phys., Condens. Matter* **20**, 252203 (2008).
- [23] J.F. Scott, M.K. Singh, R.S. Katiyar, *J. Phys., Condens. Matter* **20**, 322203 (2008).
- [24] J.F. Scott, M.K. Singh, R.S. Katiyar, *J. Phys., Condens. Matter* **20**, 425223 (2008).
- [25] S.A.T. Redfern, C. Wang, J.W. Hong, G. Catalan, J.F. Scott, *J. Phys., Condens. Matter* **20**, 452205 (2008).
- [26] S. Vijayanand, M.B. Mahajan, H.S. Potdar, P.A. Joy, *Phys. Rev. B* **80**, 064423 (2009).
- [27] J. Lu, A. Guenther, F. Schrettle, F. Mayr, S. Krohns, P. Lunkenheimer, A. Pimenov, V.D. Travkin, A.A. Mukhin, A. Loidl, *arXiv:0910.0385v1* [cond-mat.mtrl-sci] (2009).
- [28] G.D. Achenbach, W.J. James, R. Gerson, *J. Am. Ceram. Soc.* **50**, 437 (1967).
- [29] H.M. Rietveld, *J. Appl. Cryst.* **2**, 65 (1969).
- [30] J. Rodríguez-Carvajal, *Physica B* **192**, 55 (1993).
- [31] F. Kubel, H. Schmid, *Acta Cryst. B* **46**, 698 (1990).
- [32] I. Sosnowska, W. Schäfer, W. Kockelmann, K.H. Andersen, I.O. Troyanchuk, *Appl. Phys. A* **74**, S1040 (2002).
- [33] J.D. Bucci, B.K. Robertson, W.J. James, *J. Appl. Cryst.* **5**, 187 (1972).
- [34] A. Palewicz, T. Szumiata, R. Przeniosło, I. Sosnowska, I. Margiolaki, *Sol. Stat. Comm.* **140**, 359 (2006).
- [35] M. Yashima, D. Ishimura, Y. Yamaguchi, K. Ohoyama, K. Katsuhiko, *Chem. Phys. Lett.* **372**, 784 (2003).